Monthly Notices of the ROYAL ASTRONOMICAL SOCIETY **MNRASL Advance Access published October 23, 2013**

MNRASL (2013) doi:10.1093/mnrasl/slt131

Herschel observations and a model for IRAS 08572+3915: a candidate for the most luminous infrared galaxy in the local ($z < 0.2$) Universe

A. Efstathiou,[1]⋆ C. Pearson,[2,3] D. Farrah,[4] D. Rigopoulou,[2,5] J. Graciá-Carpio,[6] A. Verma,[5] H. W. W. Spoon,[7] J. Afonso,[8,9] J. Bernard-Salas,[3,10] D. L. Clements,[11] A. Cooray,[12] D. Cormier,[13] M. Etxaluze,[14] J. Fischer,[15] E. González-Alfonso,[16] P. Hurley,[17] V. Lebouteiller,[7,18] S. J. Oliver,[17] M. Rowan-Robinson[11] and E. Sturm[6]

[1]*School of Sciences, European University Cyprus, Diogenes Street, Engomi, 1516 Nicosia, Cyprus*
[2]*Space Science and Technology Department, CCLRC Rutherford Appleton Laboratory, Chilton, Didcot, Oxfordshire OX11 0QX, UK*
[3]*Astrophysics Group, Department of Physics, The Open University, Milton Keynes MK7 6AA, UK*
[4]*Department of Physics, Virginia Tech, Blacksburg, VA 24061, USA*
[5]*Oxford Astrophysics, Denys Wilkinson Building, University of Oxford, Keble Rd, Oxford OX1 3RH, UK*
[6]*Max-Planck-Institut für extraterrestrische Physik, Postfach 1312, D-85741 Garching, Germany*
[7]*Astronomy Department, Cornell University, Ithaca, NY 14853, USA*
[8]*Centro de Astronomia e Astrofísica da Universidade de Lisboa, Observatório Astronómico de Lisboa, Tapada da Ajuda, P-1349-018 Lisbon, Portugal*
[9]*Department of Physics, Faculty of Sciences, University of Lisbon, Campo Grande, P-1749-016 Lisbon, Portugal*
[10]*Institut d'Astrophysique Spatiale, Universite Paris-Sud 11, F-91405 Orsay, France*
[11]*Astrophysics Group, Imperial College London, Blackett Laboratory, Prince Consort Road, London SW7 2AZ, UK*
[12]*Department of Physics and Astronomy, University of California, Irvine, CA 92697, USA*
[13]*Institut für theoretische Astrophysik, Zentrum für Astronomie der Universität Heidelberg, Albert-Ueberle St. 2, D-69120 Heidelberg, Germany*
[14]*Departamento de Astrofísica, Centro de Astrobiología, CSIC-INTA, Torrejón de Ardoz, E-28850 Madrid, Spain*
[15]*Naval Research Laboratory, Remote Sensing Division, 4555 Overlook Ave SW, Washington, DC 20375, USA*
[16]*Departamento de Física y Matemáticas, Universidad de Alcalá de Henares, Campus Universitario, E-28871 Alcalá de Henares, Madrid, Spain*
[17]*Department of Physics and Astronomy, University of Sussex, Falmer, Brighton BN1 9QH, UK*
[18]*Laboratoire AIM, CEA/DSM-CNRS-Universite Paris Diderot, DAPNIA/Service d'Astrophysique, Saclay, F-91191 Gif-sur-Yvette Cedex, France*

Accepted 2013 September 19. Received 2013 September 17; in original form 2013 August 1

ABSTRACT

We present *Herschel* photometry and spectroscopy, carried out as part of the *Herschel* ultraluminous infrared galaxy (ULIRG) survey, and a model for the infrared to submillimetre emission of the ULIRG IRAS 08572+3915. This source shows one of the deepest known silicate absorption features and no polycyclic aromatic hydrocarbon emission. The model suggests that this object is powered by an active galactic nucleus (AGN) with a fairly smooth torus viewed almost edge-on and a very young starburst. According to our model, the AGN contributes about 90 per cent of the total luminosity of $1.1 \times 10^{13}\,L_{\odot}$, which is about a factor of 5 higher than previous estimates. The large correction of the luminosity is due to the anisotropy of the emission of the best-fitting torus. Similar corrections may be necessary for other local and high-z analogues. This correction implies that IRAS 08572+3915 at a redshift of 0.058 35 may be the nearest hyperluminous infrared galaxy and probably the most luminous infrared galaxy in the local ($z < 0.2$) Universe. IRAS 08572+3915 shows a low ratio of [C II] to IR luminosity ($\log L_{[\mathrm{C\,II}]}/L_{\mathrm{IR}} < -3.8$) and a [O I]63 μm to [C II]158 μm line ratio of about 1 that supports the model presented in this Letter.

Key words: radiative transfer – galaxies: active – galaxies: individual (IRAS 08572+3915) – infrared: galaxies.

1 INTRODUCTION

Recent results from *Herschel* surveys have shown that high-redshift ultraluminous infrared galaxies (ULIRGs; with luminosities greater than $10^{12}\,L_{\odot}$) are generally colder and less obscured than their local counterparts (Elbaz et al. 2011). This supports pre-*Herschel*

⋆ E-mail: a.efstathiou@euc.ac.cy

predictions on the basis of models of the spectral energy distributions (SEDs) of submillimetre galaxies that they have significant contributions to their luminosity from cirrus or cold diffuse dust in the galaxy (Efstathiou & Rowan-Robinson 2003; Efstathiou & Siebenmorgen 2009). The other surprising result of *Herschel* and *Spitzer* surveys, however, is that there are large numbers of distant ULIRGs that show stronger silicate absorption than the majority of local ULIRGs (Rowan-Robinson et al. 2010; Sajina et al. 2012).

IRAS 08572+3915 surely ranks as one of the most peculiar local ULIRGs but may be typical of the highly obscured distant ULIRGs. It shows extremely deep silicate absorption features both at 9.7 (silicate strength ~ -4; see equation 1 of Spoon et al. 2007) and 18 μm (Dudley & Wynn-Willams 1997), which are deeper than those of the prototypical ULIRG Arp 220, and at the same time it shows no evidence of polycyclic aromatic hydrocarbon (PAH) emission features either in the mid-infrared or at 3.3 μm (Imanishi et al. 2008; Veilleux et al. 2009). This has been interpreted as evidence that IRAS 08572+3915 is powered by an active galactic nucleus (AGN), but results from calculations of the emission from clumpy tori, which are favoured on theoretical grounds (e.g. Krolik & Begelman 1988), do not show silicate absorption features as deep as those observed in IRAS 08572+3915 (Levenson et al. 2007). This is because in a clumpy medium, even in the case where we view the torus edge-on, it is possible to see the inner hot dust through holes in the cloud distribution and this has the effect of filling in the absorption features produced by foreground clumps. So for the mid-IR emission from IRAS 08572+3915 to be powered by an AGN, the torus must have either an unusually high filling factor, or be fairly smooth.

Spoon et al. (2007) presented a diagnostic diagram that plots the silicate strength of about 200 infrared galaxies and AGN versus their 6.2 μm PAH equivalent width. Rowan-Robinson & Efstathiou (2009) showed that the distribution of galaxies on the diagram of Spoon et al. can be understood in terms of the starburst models of Efstathiou, Rowan-Robinson & Siebenmorgen (2000, hereafter referred to as ERRS00 models) and the AGN torus models of Efstathiou & Rowan-Robinson (1995). The diagonal locus on the diagram can be explained by the evolution of the SED of the starbursts in the age range 0–72 Myr, and the horizontal locus can be explained by mixing of starburst and AGN torus emission. Rowan-Robinson & Efstathiou (2009) suggested that objects, such as IRAS 08572+3915, that are located at the upper tip of the diagonal locus in class 3A of Spoon et al., and which show very deep silicate absorption and no PAH features, could be either AGN with a fairly smooth edge-on torus or very young starbursts. The far-infrared to submillimetre colours predicted by these two models are however distinctly different so modelling of the complete SEDs with radiative transfer models offers the possibility of breaking the degeneracy.

This is one of a series of papers that discuss results from an analysis of the data collected by the *Herschel* ULIRG survey (HERUS; Farrah et al. 2013). As part of this survey, 43 ULIRGs have been observed in spectroscopic and photometric mode using the SPIRE (Griffin et al. 2010) and PACS (Poglitch et al. 2010) instruments on board *Herschel*. In this Letter, we use HERUS data, and data collected as part of the SHINING program (Sturm et al. 2010), as well as radiative transfer models for starburst and AGN torus emission to shed light on the origin of the luminosity of IRAS 08572+3915. Understanding this object is important as it could serve as a template for objects with deep silicate absorption that reside at high redshift. In Section 2, we describe the *Herschel* data; in Section 3, we describe the models; and in Section 4, we present the best-fitting model and discuss our results. A flat Universe is assumed with $\Lambda = 0.73$ and $H_0 = 71 \mathrm{km\,s^{-1}\,Mpc^{-1}}$.

2 DATA

IRAS 08572+3915 at a redshift of 0.058 35 was observed by the *Herschel Space Observatory* (Pilbratt et al. 2010) on 2011 October 10 with the SPIRE Photometer (Griffin et al. 2010). The photometer observations were made in small map mode in the PSW (250 μm), PMW (350 μm) and PLW (500 μm) bands. The observation was processed using version 8 of the *Herschel* Common Science System *Herschel Interactive Processing Environment* (HIPE; Ott 2010) using the standard user pipeline (Dowell et al. 2010), with default values for all tasks utilizing the SPIRE calibration tree version 8.1. Standard median baseline removal was made to create the final images using the naive mapper task. Photometry of the source was made using the SPIRE timeline source fitter task in HIPE which fits a 2D Gaussian to the timeline data at the coordinates of the source. We assumed full width at half-maximum of 18.15, 25.2, 36.9 arcsec for the PSW, PMW, PLW bands, respectively. The background was measured within an annulus between 300 and 350 arcsec and then an elliptical Gaussian function was fitted to both the central 22, 32, 40 arcsec (for the PSW, PMW, PLW bands, respectively) and the background annulus. The output is the fitted flux, RA, Dec. and associated errors. The fitted fluxes obtained from the source fitter are given in Table 1.

IRAS 08572+3915 was observed with the SPIRE Fourier Transform Spectrometer (Griffin et al. 2010) on 2011 November 7. The observation was made in high-resolution point source mode covering the entire submillimetre spectrum in two detector arrays from 194–313 μm (SSW) and 303–671 μm (SLW). The spectrometer observations were also reduced with the standard HIPE version 11 spectrometer user pipeline (Fulton et al. 2010), processing just the central detectors of each array to produce the final calibrated point source spectra. The standard pipeline subtracts the telescope background emission using an emission model derived from the measured primary and secondary mirror temperatures during the observation. This process leaves an uncertainty of $\sim$1.5 Jy, significant for faint sources. A more accurate background subtraction was therefore made using the off-axis detectors in each array to measure areas of dark sky. The resulting spectrum for IRAS 08572+3915 shows three ^{12}CO lines (^{12}CO(11–10) 237 μm, ^{12}CO(10–9) 260 μm and ^{12}CO(9–8) 289 μm) and the [C I] line at a rest wavelength of 607 μm. More details about these results will be given in a forthcoming paper.

Table 1. SPIRE photometry and PACS spectroscopy for IRAS 08572+3915.

Photometry		
wavelength	Flux (Jy)	Error (mJy)
250 μm	0.532	4.1
350 μm	0.168	4.0
500 μm	0.056	4.8
Spectroscopy		
wavelength	Intensity (W m^{-2})	Error (W m^{-2})
[O I] 63 μm	1.18×10^{-16}	1.74×10^{-17}
[O III] 88 μm	5.73×10^{-17}	2.63×10^{-18}
[C II] 158 μm	1.12×10^{-16}	3.00×10^{-18}

We also obtained PACS spectroscopy of IRAS 08572+3915 as part of the SHINING program (PI: Sturm). The data reduction of the PACS spectroscopic observations was carried out using the standard *Herschel* data reduction pipeline included in HIPE 6.0, with some modifications introduced to correct for small offsets in the continuum of the spectral pixels. The spectrum was normalized to the telescope background and recalibrated with a reference Neptune spectrum obtained during the *Herschel* PV phase. With this method, errors in the absolute flux calibration are generally lower than 20 per cent. The galaxy is detected in three far-infrared lines whose fluxes are given in Table 1.

IRAS 08572+3915 was one of the ULIRGs observed in the *Spitzer* Guaranteed Time Observation ULIRG project (PID 105; PI: Houck) and its IRS spectrum first appeared in Spoon et al. (2006). In the analysis that follows, we will use the IRS spectrum resulting from the data processing of Wang et al. (2011). Similar results are obtained by using the spectrum available by the CASSIS data base (Lebouteiller et al. 2011).

3 RADIATIVE TRANSFER MODELS

Several models for the infrared emission of starburst galaxies have been developed (Rowan-Robinson & Crawford 1989; Rowan-Robinson & Efstathiou 1993; Krügel & Siebenmorgen 1994; Silva et al. 1998; Tagaki, Arimoto & Hanami et al. 2003; Dopita et al. 2005; Siebenmorgen & Krügel 2007). Efstathiou et al. (2000) presented a starburst model that combined the stellar population synthesis model of Bruzual & Charlot, radiative transfer that included the effect of small grains and PAHs, and a simple scheme for the evolution of the molecular clouds that constitute the starburst. The model predicts the SEDs of starburst galaxies from the ultraviolet to the millimetre for different ages of the starburst and different initial optical depths of the molecular clouds. The ERRS00 model uniquely predicts that young starbursts have small PAH equivalent widths and deep silicate absorption features whereas older starbursts have stronger PAH features and more shallow silicate absorption features. In this Letter, we use a grid of starburst models which have been computed with the method of ERRS00 but with a revised dust model (Efstathiou & Siebenmorgen 2009). In this grid of models, we vary the initial optical depth in the V band of the molecular clouds ($\tau_V = 50$, 75, and 100) and the age of the starburst in the range 0–70 Myr in steps of 5 Myr.

Radiative transfer models of the torus in AGN have been presented by Pier & Krolik (1992), Granato & Danese (1994), Nenkova, Ivezic & Elitzur (2002), Nenkova et al. (2008), Dullemond & van Bemmel (2005), Hönig et al. (2006), Schartmann et al. (2008), Stalevski et al. (2012) and Heymann & Siebenmorgen (2012). Efstathiou & Rowan-Robinson (1995) considered three different types of geometry for the torus and concluded that the geometry that best fitted the observational constraints was that of tapered discs (whose thickness increases linearly with distance from the central source in the inner part of the disc but tapers off to a constant height in the outer part). The tapered disc models consider a distribution of grain species and sizes, multiple scattering and a smooth density distribution that follows r^{-1} where r is the distance from the central source. The models have been quite successful in fitting the SEDs of AGN even in cases where mid-infrared spectroscopy is available (Efstathiou, Hough & Young 1995; Alexander et al. 1999; Ruiz et al. 2001; Farrah et al. 2002, 2003, 2012; Verma et al. 2002; Efstathiou & Siebenmorgen 2005; Efstathiou et al. 2013).

In this Letter, we use a grid of tapered disc models computed with the method of Efstathiou & Rowan-Robinson (1995) and described in more detail in Efstathiou et al. (2013). In this grid of models, we consider five discrete values for the equatorial 1000 Å optical depth ($\tau_{UV}^{\rm eq} = 250$, 500, 750, 1000, 1250; $\tau_{UV}^{\rm eq} \approx 5\tau_V^{\rm eq}$), three values for the ratio of outer to inner disc radii ($r_2/r_1 = 20$, 60, 100) and four values for the half-opening angle of the disc ($\Theta_0 = 30^\circ$, 45°, 60° and 75°; Θ_1 as defined by Efstathiou & Rowan-Robinson is equal to $90 - \Theta_0$). The spectra are computed for 37 inclinations i which are equally spaced in the range 0°–90°. The grids of tapered disc and starburst models discussed above are available from AE on request.[1]

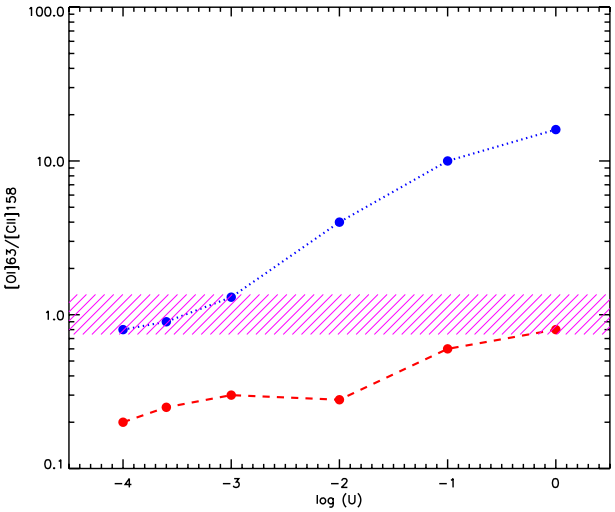

Figure 1. Line ratios predicted from CLOUDY runs with different ionization parameters U. The dotted blue line corresponds to an AGN spectrum whereas the dashed red line corresponds to a zero-age starburst computed with the Bruzual & Charlot (2003) models and a Salpeter IMF. The magenta shaded region indicates the measured [O I]63 μm/[C II]158 μm ratio and its 2σ uncertainty.

4 RESULTS AND DISCUSSION

In Fig. 1, we compare the observed [O I]63 μm to [C II]158 μm line ratio with photoionization models computed with CLOUDY (Ferland et al. 1998). We have computed models that assume different ionization parameters U and two different source spectra: an AGN spectrum (shown with the blue dashed line in Fig. 1) and a young starburst spectrum that assumes a zero-age burst of star formation (red dotted line). The young starburst spectrum, which is identical with the source spectrum that is assumed by the dust radiative transfer model (see next paragraph), is obtained from the tables of Bruzual & Charlot (2003) for a Salpeter initial mass function (IMF) and solar metallicity. In all CLOUDY runs, we assume a density at the illuminated face of the cloud of 10^3 cm^{-3} and a total column density of 2×10^{23} cm^{-2}.

It is clear from Fig. 1 that the observed line ratio is consistent with either an AGN spectrum with a low-ionization parameter or a young starburst spectrum with a high-ionization parameter. Another indicator of activity in galaxies is the ratio of [C II] to IR luminosity. IRAS 08572+3915 shows a low ratio ($\log L_{\rm [C\,II]}/L_{\rm IR} = -3.8$ assuming conservatively that $L_{\rm IR} = 1.5 \times 10^{12}\,{\rm L}_\odot$) which places it well in the range shown by systems dominated by an AGN (Abel et al. 2009; Sargsyan et al. 2012). Detailed modelling of the PACS and SPIRE line observations will be presented in a future paper.

[1] Email: a.efstathiou@euc.ac.cy

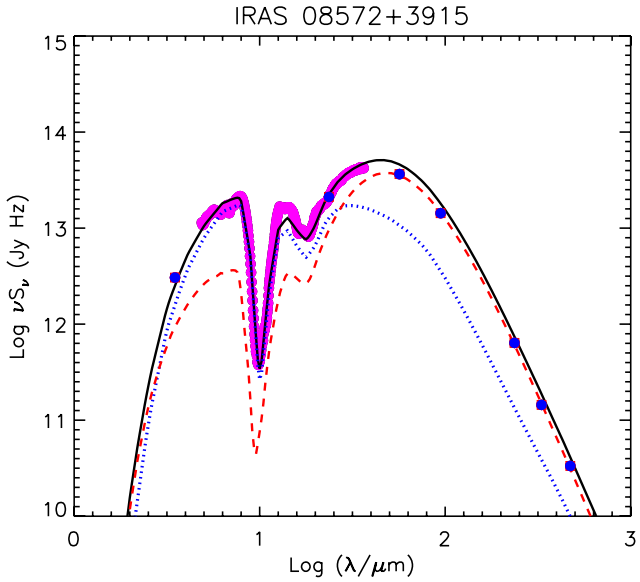

Figure 2. Fit to the SED of IRAS 08572+3915 with a smooth edge-on torus (blue dotted line) and a young starburst (red dashed line). The total emission is given by the black solid line. Broad-band data (blue filled circles) are from this work, Carico et al. (1988) and IRAS. The *Spitzer*/IRS spectrum (Wang et al. 2011) is shown in magenta.

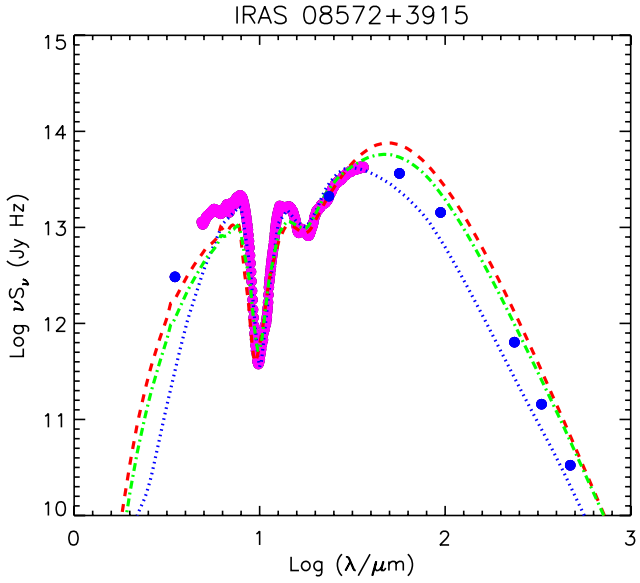

Figure 3. Best-fitting models to the SED of IRAS 08572+3915 with pure smooth torus (blue dotted line), pure clumpy torus (green dot dashed line) and pure starburst (red dashed line). The data are the same as those plotted in Fig. 2.

We can now combine the submillimetre photometry presented here with the *Spitzer* IRS spectrum from 5 to 35 μm, *IRAS* data and near-IR photometry to get another constraint on the power source. In Fig. 2, we present our best-fitting model for the SED of IRAS 08572+3915 which is obtained by finding the combination of starburst and smooth AGN torus models that minimizes χ^2. Our fitting code can return a pure AGN or a pure starburst model if it is the preferred solution. We find that a pure AGN model (shown in Fig. 3) has a reduced $\chi^2_{\rm min}$ of 9.1 whereas the corresponding value for a pure starburst model is 15.8. The $\chi^2_{\rm min}$ of the AGN/starburst combination is 3.25. The best-fitting starburst model has an age of 0 Myr and an initial optical depth of the molecular clouds that constitute the starburst of 75. The best-fitting torus model assumes $r_2/r_1 = 60$, $\tau^{\rm eq}_{\rm UV} = 500$, $\Theta_0 = 75^\circ$ and $i = 88^\circ$. Our grid of starburst and AGN torus models is fairly crude so we can get sensible uncertainties only on the inclination and age of the starburst. We find that even for $\Delta\chi^2 = 30$, the uncertainty in inclination is 5° and in age is 5 Myr. The 1–1000 μm starburst luminosity is predicted to be $10^{12}\,{\rm L}_\odot$ and the AGN *apparent* luminosity $6.6 \times 10^{11}\,{\rm L}_\odot$. Because of the anisotropy of the emission of the torus, the luminosity of the AGN must be multiplied by the anisotropy correction factor A of 14.6 to give the intrinsic luminosity of $9.6 \times 10^{12}\,{\rm L}_\odot$ (Efstathiou 2006). Assuming there is no processing of the AGN and starburst emission by the host galaxy, the total luminosity of the system is therefore predicted to be $1.1 \times 10^{13}\,{\rm L}_\odot$, 90 per cent of which is due to the AGN. According to Rowan-Robinson & Wang (2010; see their fig. 1), the nearest *IRAS* galaxy that exceeds the $10^{13}\,{\rm L}_\odot$ threshold, and is therefore classified as a hyperluminous infrared galaxy, lies at $z > 0.3$. Other *IRAS* galaxies within $z < 0.3$ may need a correction of their luminosity because of anisotropic torus emission but such high anisotropy corrections are only expected for AGN with very deep silicate absorption features. IRAS 08572+3915 has the second deepest silicate feature in the sample of Spoon et al. (2007), just shallower than that of IRAS 01298−0744 at a redshift of 0.136 18 which is also the galaxy with the highest silicate optical depth in the sample of Veilleux et al. (2009). Although according to our model, IRAS 01298−0744 also needs a large anisotropy correction, its intrinsic luminosity is estimated to be only about $5 \times 10^{12}\,{\rm L}_\odot$. IRAS 08572+3915 may therefore be the nearest hyperluminous infrared galaxy and the most luminous infrared galaxy in the local ($z < 0.2$) Universe. The solution found here is different from that found by Farrah et al. (2003) who only considered broad-band data and estimated that the starburst in IRAS 08572+3915 is about a factor of 2 more luminous than the AGN and the galaxy has a total IR luminosity of $1.5 \times 10^{12}\,{\rm L}_\odot$.

To test whether clumpy torus models can match the SED of IRAS 08572+3915, we have compared its SED with the models of Stalevski et al. (2012). We find that even the AGN torus models with the most optically thick clumps ($\tau_{9.7\,\mu{\rm m}} = 10$) when observed edge-on fail to match the deep silicate absorption feature of IRAS 08572+3915 ($\chi^2_{\rm min} = 28.8$, see Fig. 3). A combined clumpy torus and starburst fit gives a $\chi^2_{\rm min}$ of 13.3.

Determining the true distribution of dust in the torus (i.e. whether it is smooth, filamentary, clumpy or two-phase medium) is important not only for understanding the physics of the torus but also for estimating the intrinsic luminosity of AGNs from the observed one. Clumpy tori generally emit much more isotropically than smooth tori (Nenkova et al. 2008; Hönig et al. 2011). Hönig et al. (2011) estimate that at 15 μm type 1 AGN are only a factor of 1.4 more luminous than type 2 AGN but according to the best-fitting torus model presented here for IRAS 08572+3915, at 15 μm the ratio of face-on/edge-on emission is of the order of 10 and this is what makes this and other similar objects so intrinsically luminous.

ACKNOWLEDGEMENTS

Herschel is an ESA space observatory with science instruments provided by European-led Principal Investigator consortia and with important participation from NASA. Basic research in IR astronomy at NRL is funded by the US ONR. JF also acknowledges support from the NHSC. JBS acknowledges support from a Marie Curie Intra-European Fellowship within the 7th European Community

Framework Program under project number 272820. EG-A is a Research Associate at the Harvard–Smithsonian Center for Astrophysics, and thanks the Spanish Ministerio de Economía y Competitividad for support under projects AYA2010-21697-C05-0 and FIS2012-39162-C06-01. ME acknowledges support from ASTROMADRID (grant S2009ESP-1496), ASTROMOL (CSD2009-00038) and the Spanish MINECO (AYA2009-07304 and AYA2012-32032). JA acknowledges support from the Science and Technology Foundation (FCT, Portugal) through the research grants PTDC/CTE-AST/105287/2008, PEst-OE/FIS/UI2751/2011 and PTDC/FIS-AST/2194/2012. We also thank an anonymous referee for his comments and suggestions.

REFERENCES

Abel N. P., Dudley C., Fischer J., Satyapal S., van Hoof P. A. M., 2009, ApJ, 701, 1147
Alexander D. M., Efstathiou A., Hough J. H., Aitken D. K., Lutz D., Roche P. F., Sturm E., 1999, MNRAS, 310, 78
Bruzual A. G., Charlot S., 2003, MNRAS, 344, 1000
Carico D. P., Sanders D. B., Soifer B. T., Elias J. H., Matthews K., Neugebauer G., 1988, AJ, 95, 356
Dopita M. A. et al., 2005, ApJ, 619, 755
Dowell C. et al., 2010, Proc. SPIE, 7731, 773136
Dudley C. C., Wynn-Willams C. G., 1997, ApJ, 488, 720
Dullemond C. P., van Bemmel I. M., 2005, A&A, 436, 47
Efstathiou A., 2006, MNRAS, 371, L70
Efstathiou A., Rowan-Robinson M., 1995, MNRAS, 273, 649
Efstathiou A., Rowan-Robinson M., 2003, MNRAS, 343, 322
Efstathiou A., Siebenmorgen R., 2005, A&A, 439, 85
Efstathiou A., Siebenmorgen R., 2009, A&A, 502, 541
Efstathiou A., Hough J. H., Young S., 1995, MNRAS, 277, 1134
Efstathiou A., Rowan-Robinson M., Siebenmorgen R., 2000, MNRAS, 313, 734
Efstathiou A., Christopher N., Verma A., Siebenmorgen R., 2013, MNRAS, in press doi:10.1093/mnras/stt1695
Elbaz D. et al., 2011, A&A, 533, A119
Farrah D., Serjeant S., Efstathiou A., Rowan-Robinson M., Verma A., 2002, MNRAS, 335, 1163
Farrah D., Afonso J., Efstathiou A., Rowan-Robinson M., Fox M., Clements D., 2003, MNRAS, 343, 585
Farrah D. et al., 2012, ApJ, 745, 178
Farrah D. et al., 2013, ApJ, 776, 38
Ferland G. J., Korista K. T., Verner D. A., Ferguson J. W., Kingdon J. B., Verner E. M., 1998, PASP, 110, 761
Fulton T. et al., 2010, Proc. SPIE, 7731, 773134
Granato G. L., Danese L., 1994, MNRAS, 268, 235
Griffin M. et al., 2010, A&A, 518, 3
Heymann F., Siebenmorgen R., 2012, ApJ, 751, 27
Hönig S. F., Beckert T., Ohnaka K., Weigelt G., 2006, A&A, 452, 459
Hönig S. F., Leipski C., Antonucci R., Haas M., 2011, ApJ, 736, 6
Imanishi M., Nakagawa T., Ohyama Y., Shirahata M., Wada T., Onaka T., Oi N., 2008, PASJ, 60, 489
Krolik J. H., Begelman M. C., 1988, ApJ, 329, 702
Krügel E., Siebenmorgen R., 1994, A&A, 282, 407
Lebouteiller V., Barry D. J., Spoon H. W. W., Bernard-Salas J., Sloan G. C., Houck J. R., Weedman D., 2011, ApJS, 196, 8
Levenson N. A., Sirocky M. M., Hao L., Spoon H. W. W., Marshall J. A., Elitzur M., Houck J. R., 2007, ApJ, 654, L45
Nenkova M., Ivezic Z., Elitzur M., 2002, ApJ, 570, L9
Nenkova M., Sirocky M. M., Nikutta R., Ivezic Z., Elitzur M., 2008, ApJ, 685, 160
Ott S., 2010, in Mizumoto Y., Morita K.-I., Ohishi M., eds, ASP Conf. Ser. Vol. 434, Astronomical Data Analysis Software and Systems XIX. Astron. Soc. Pac., San Francisco, p. 139
Pier E. A., Krolik J. H., 1992, ApJ, 401, 99
Pilbratt G. L. et al., 2010, A&A, 518, 1
Poglitch A. et al., 2010, A&A, 518, L2
Rowan-Robinson M., Crawford J., 1989, MNRAS, 238, 523
Rowan-Robinson M., Efstathiou A., 1993, MNRAS, 263, 675
Rowan-Robinson M., Efstathiou A., 2009, MNRAS, 399, 615
Rowan-Robinson M., Wang L., 2010, MNRAS, 406, 720
Rowan-Robinson M. et al., 2010, MNRAS, 409, 2
Ruiz M., Efstathiou A., Alexander D. M., Hough J., 2001, MNRAS, 325, 995
Sajina A., Yan L., Fadda D., Sasyra K., Huynh M., 2012, ApJ, 757, 13
Sargsyan L. et al., 2012, ApJ, 755, 171
Schartmann M., Meisenheimer K., Camenzind M., Wolf S., Tristram K. R. W., Henning T., 2008, A&A, 482, 67
Siebenmorgen R., Krügel E., 2007, A&A, 461, 445
Silva L., Granato G. L., Bressan A., Danese L., 1998, ApJ, 509, 103
Spoon H. W. W. et al., 2006, ApJ, 638, 759
Spoon H. W. W., Marshall J. A., Houck J. R., Elitzur M., Hao L., Armus L., Brandl B. R., Charmandaris V., 2007, ApJ, 654, L49
Stalevski M., Fritz J., Baes M., Nakos T., Popovic L. C., 2012, MNRAS, 420, 2756
Sturm E. et al., 2010, A&A, 518, L36
Tagaki T., Arimoto N., Hanami H., 2003, MNRAS, 340, 813
Veilleux S. et al., 2009, ApJS, 182, 628
Verma A., Rowan-Robinson M., McMahon R., Efstathiou A., 2002, MNRAS, 335, 574
Wang L., Farrah D., Connolly B., Connolly N., Lebouteiller V., Oliver S., Spoon H., 2011, MNRAS, 411, 1809

This paper has been typeset from a TEX/LATEX file prepared by the author.